



CHORUS

This is the accepted manuscript made available via CHORUS. The article has been published as:

Chemical doping and high-pressure studies of layered β -PdBi₂ single crystals

Kui Zhao, Bing Lv, Yu-Yi Xue, Xi-Yu Zhu, L. Z. Deng, Zheng Wu, and C. W. Chu

Phys. Rev. B **92**, 174404 — Published 4 November 2015

DOI: [10.1103/PhysRevB.92.174404](https://doi.org/10.1103/PhysRevB.92.174404)

Chemical doping and high pressure studies of layered β -PdBi₂ single crystals

Kui Zhao¹, Bing Lv^{1,*}, Yu-Yi Xue¹, Xi-Yu Zhu^{1,2},
Liangzi Deng¹, Zheng Wu¹ and C. W. Chu^{1,3}

¹ Texas Center for Superconductivity and Department of Physics, University of Houston, Houston, TX 77204-5002.

² Department of Physics, Nanjing University, Nanjing, China.

³ Lawrence Berkeley National Laboratory, Berkeley CA 94720

* Current address: Department of Physics, University of Texas at Dallas, Richardson, TX 75080. Email: blv@utdallas.edu

Abstract:

We have systematically grown large single crystals of layered compound β -PdBi₂, both the hole-doped PdBi_{2-x}Pb_x and the electron-doped Na_xPdBi₂, and studied their magnetic and transport properties. Hall-effect measurement on PdBi₂, PdBi_{1.8}Pb_{0.2}, and Na_{0.057}PdBi₂ shows that the charge transport is dominated by electrons in all of the samples. The electron concentration is substantially reduced upon Pb-doping in PdBi_{2-x}Pb_x and increased upon Na-intercalation in Na_xPdBi₂, indicating the effective hole-doping by Pb and electron-doping by Na. We observed a monotonic decrease of superconducting transition temperature (T_c) from 5.4K in undoped PdBi₂ to less than 2K for $x > 0.35$ in hole-doped PdBi_{2-x}Pb_x. Meanwhile, a rapid decrease of T_c with the Na intercalation is also observed in the electron-doped Na_xPdBi₂, which is in disagreement with the theoretical expectation. In addition, both the magnetoresistance and Hall resistance further reveal evidence for a possible spin excitation associated with Fermi surface reconstruction ~ 50 K in the Na-intercalated PdBi₂ sample. The complete phase diagram is thus established from hole-doping to electron-doping. Meanwhile, high pressure study of the undoped PdBi₂ shows that the T_c is linearly suppressed under pressure with a dT_c/dP coefficient of -0.28K/GPa.

Introduction:

Low dimensional compounds, with simple structure building motifs and weak bonding force between layers, have generated much research interest within condensed matter physics over the past several decades. These low dimensional materials have displayed a variety of unusual physical phenomena such as charge density waves in transition metal chalcogenides¹⁻²; spin density waves in parent Fe-pnictide superconductors³⁻⁴; topological order in Bi₂Se₃⁵⁻⁶; and superconductivity in many compounds such as MgB₂⁷, doped ZrNCl⁸, etc. In the binary Pd-Bi alloy family, several phases with different structures have been studied⁹ in the past, in which the PdBi₂ is found to crystalize in two different layered structures with a low temperature α -phase below 380°C and a high temperature β -phase between 380°C and 490°C¹⁰. The α -PdBi₂ crystalizes in a layered monoclinic (c2/m) structure with a six-coordinated PdBi₆ building motif, while the β -PdBi₂ forms a

layered tetragonal CuZr_2 -type structure ($I4/mmm$) with an eight-coordinated PdBi_8 building motif. Every four Bi-atoms in the $\beta\text{-PdBi}_2$ are face-shared with the neighboring CsCl-type PdBi_8 motif and therefore form a $\text{PdBi}_{8/4}=\text{PdBi}_2$ layer. The resulting PdBi_2 layers are packed alternately and form the body centered tetragonal structure, as shown in the inset of Fig. 1(a). The interlayer spacing between the alternating PdBi_2 layers is rather large, with interlayer Bi-Bi distance of $\sim 3.8\text{\AA}$, indicating that there is no effective bonding between those layers. Various phases in the Pb-Bi system have been identified as superconductors¹¹, such as $\alpha\text{-PdBi}$ with $T_c \sim 3.8\text{K}$, $\alpha\text{-PdBi}_2$ with $T_c \sim 1.73\text{K}$, $\beta\text{-PdBi}_2$ with $T_c \sim 4.25\text{K}$, and $\text{Pd}_{2.5}\text{Bi}_{1.5}$ with $T_c \sim 3.7\text{-}4\text{K}$. Early studies showed that $\beta\text{-PdBi}_2$ had the highest T_c among them, 4.25K ¹¹, and it was recently shown that the T_c could be further raised to 5.4K by improving the sample quality¹². However, neither details of chemical doping nor high pressure effect have been studied previously in $\beta\text{-PdBi}_2$. The prior specific heat and STM studies on $\beta\text{-PdBi}_2$ suggest that it is a multi-band superconductor^{12,13}, which is in agreement with the results from first principle calculations¹⁴. Theoretical calculation shows that the density of states (DOS) around the Fermi level is dominated by the Pd $4d$ and Bi $6p$ states, and that the Fermi level is located on a positive slope below a DOS peak. Therefore, hole doping is expected to shift the Fermi level away from the DOS peak, resulting in a decrease of the DOS at the Fermi level while electron doping will increase it. Therefore, one would expect a decrease of T_c upon hole doping and an increase of T_c under electron doping. Under this motivation, we decided to carry out systematic hole doping (substitution of Bi with Pb) and electron doping (Na-intercalation) studies on the $\beta\text{-PdBi}_2$ system. However, we found that the T_c was suppressed in both cases, the reasons for which will be discussed in this paper. Meanwhile, the high pressure study was also carried out on the $\beta\text{-PdBi}_2$ single crystal and we observed a suppression of T_c upon applied pressure with a dT_c/dP coefficient of -0.28K/GPa . The phase diagrams, both upon chemical doping and under high pressure, are presented.

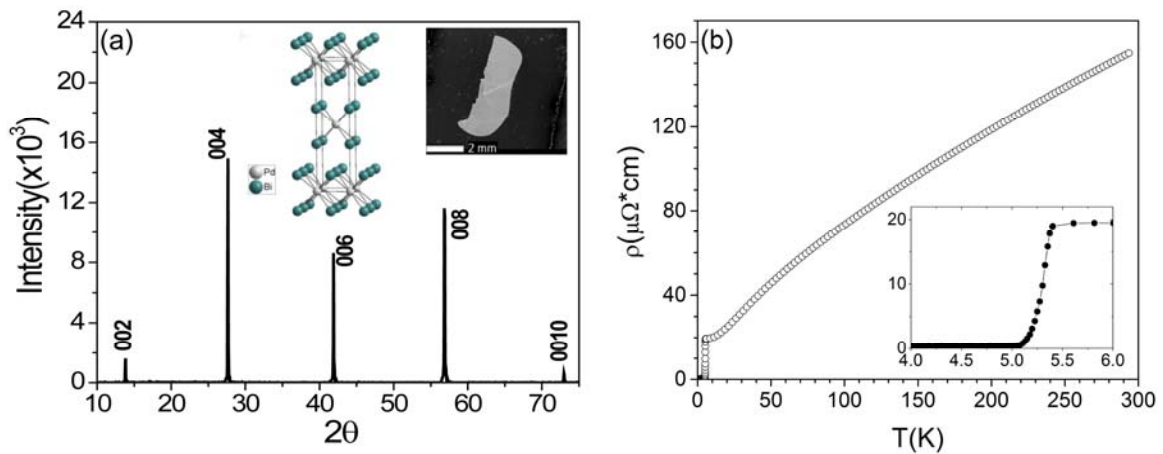


Fig.1 (a) XRD pattern of $\beta\text{-PdBi}_2$ with preferred orientation along c axis; the inset shows the crystal structure and one representative crystal SEM image. (b) Resistivity of $\beta\text{-PdBi}_2$ from 2K to 300K ; the inset displays resistivity data between 4K and 6K .

Experimental details:

The β -PdBi₂ single crystals were synthesized through a melt-growth method. Stoichiometric amounts of Pd and Bi grains were sealed in an evacuated quartz tube, which was heated up to 700°C, kept for 10 hours, and then slowly cooled to 450°C over 30 hours. In order to retain the β -phase, the tube was then quenched in iced water directly from 450°C. Similarly, a series of PdBi_{2-x}Pb_x ($x= 0.0, 0.08, 0.15, 0.20, 0.28, 0.35, 0.40, 0.60, 0.80,$ and 1.0) crystals was attempted to be grown with stoichiometric amounts of Pd, Bi, and Pb. In addition, the Na_xPdBi₂ compounds were grown by mixing Na and previously obtained PdBi₂ precursor, followed by the same synthetic condition but using a carbon-coated quartz tube to prevent the possible reaction of sodium with the quartz tube at high temperature. The carbon coating of the quartz tube was found to be intact after the synthesis, indicating the success of the growth. X-ray powder diffraction was performed on the powdered Pb-doped single crystals at room temperature from 10 to 90 degrees using a Panalytical X'pert Diffractometer. The actual chemical compositions were determined by wavelength-dispersive spectrometry (WDS) on a JEOL JXA-8600 electron microprobe analyzer. At least 6 well separated points across the crystal were measured to confirm the homogeneity of the dopants. The dc magnetic susceptibility was measured as a function of temperature $\chi(T)$ using a Quantum Design Magnetic Property Measurement System (MPMS) down to 2 K. Electrical resistivity as a function of temperature $\rho(T)$ and field $\rho(H)$ was measured by employing a standard 4-probe method using a Linear Research LR400 ac bridge operated at 15.9 Hz in a Quantum Design Physical Property Measurement System (PPMS) up to 7 T and down to 1.9 K. High pressure resistivity measurements with a 4-lead technique using the LR-400 Resistance Bridge were made in a Be-Cu pressure cell using Fluorinert FC77 as the pressure media. A lead manometer was used to measure the pressure *in situ* with the LR400 Inductance Bridge¹⁵. The Hall resistivity measurements were performed in the PPMS system with field up to 5T using the 5-lead technique, which balanced the longitudinal resistance to be close to zero.

Results and discussions:

β -PdBi₂ single crystals with shining metallic luster, typical size of 5mm, and preferred orientation along the *c*-axis after cleavage, could be obtained through the melt-growth technique, as shown in Fig. 1(a). The calculated lattice parameter *c* [12.963(3)Å] is consistent with previous reports¹². A representative SEM image of the undoped β -PdBi₂ single crystal is also shown as the inset of Fig. 1(a). Both resistivity and magnetization measurements have shown that the superconducting transition temperature of the as-grown β -PdBi₂ crystal is 5.4K, indicating the improved quality of the grown crystals as also pointed out by previous reports¹². The resistivity curve exhibits a hump below 150K and a minor downturn around 50K, as shown in Fig. 1(b), suggesting possible strong electron/spin correlation in this compound.

Fig. 2 shows the powder XRD patterns with Miller indices of the crushed crystals for the Pb-doped PdBi_{2-x}Pb_x ($x=0.08, 0.15, 0.20, 0.28, 0.35,$ and 0.40) samples. Except for a few minor peaks of the α -phase present at low doping level, namely $x=0.08$, all of the peaks are well indexed into the β -PdBi₂-type body centered tetragonal structures in all of the

samples with different doping levels. These crystals are quite stable outside of the glove box for several months. Due to the close radius sizes between the Pb and Bi, the change of lattice parameter upon Pb doping is very small, and a gradual decrease of the lattice parameter from 12.963(3)Å for $x=0$ to 12.940(2)Å for $x=0.4$ is observed, but the overall lattice parameters change is less than 0.2%. To further confirm the homogeneity of the doped samples and establish the actual doping levels, we performed chemical analyses through WDS measurements on the single crystals. The Pb-concentration is homogenous throughout the whole samples, indicating the formation of solid solutions for these Pb-doped samples. The actual Pb-doping levels are $x=0.08(2)$, $0.14(2)$, $0.19(2)$, $0.27(2)$, $0.34(1)$, and $0.39(1)$, for the nominal compositions of $x = 0.08, 0.15, 0.20, 0.28, 0.35,$ and 0.40 in $\text{PdBi}_{2-x}\text{Pb}_x$, respectively. The results show that the actual doping levels are very close to the nominal compositions. Some extra impurity peaks belonging to the α - PdBi_2 monoclinic phase emerge at the doping level $x=0.60$ from X-ray powder diffraction and become more dominant with further Pb-doping. At the doping level of $x=1.00$, the XRD pattern shows the nearly pure phase of α - PdBi_2 -type structure with no detectable β phase, implying the solubility limit of the tetragonal β - $\text{PdBi}_{2-x}\text{Pb}_x$ phase at this high doping level.

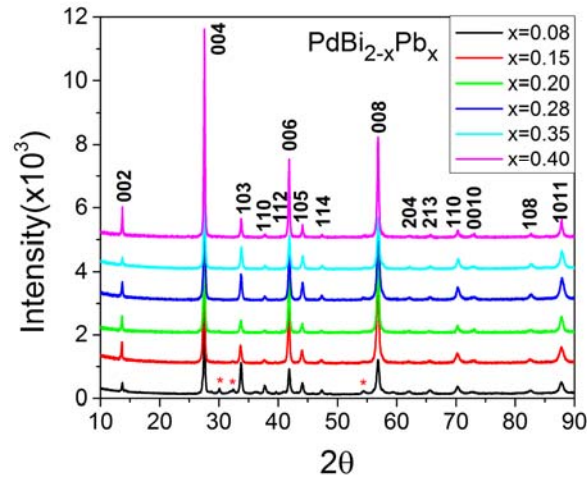


Fig.2 The powder X-ray diffraction patterns of $\text{PdBi}_{2-x}\text{Pb}_x$ with Miller indices. The patterns are vertically offset for better clarity. Some minor impurity peaks from α -phase are marked as *.

Systematic resistivity and magnetization measurements were carried out for all samples with different doping levels. As shown in Fig. 3(a), the superconducting transition temperature T_c of $\text{PdBi}_{2-x}\text{Pb}_x$ continuously decreases upon Pb substitution, from 5.4K for $x=0$, to 4.9K for $x=0.08$, 4.4K for $x=0.15$, 3.8K for $x=0.20$, 2.5K for $x=0.28$, and 2.2K for $x=0.35$. The sample eventually becomes non-superconducting above 2K when the doping level reaches $x=0.40$. The superconducting transition width (10%–90% resistivity drop) is rather narrow (less than 0.3 K) in all samples, indicating the good quality of the doped samples.

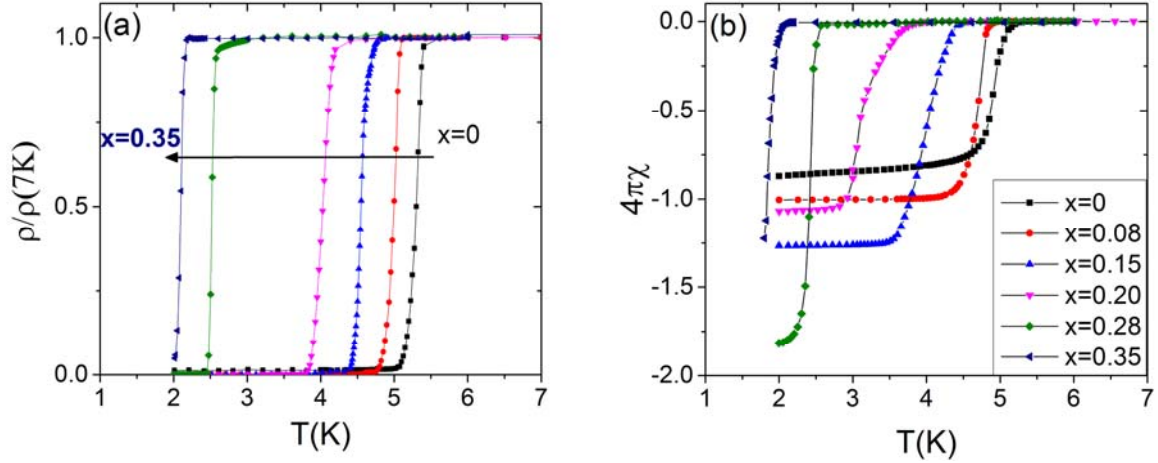


Fig.3 The resistivity (a) and magnetic susceptibility (b) data under $H=2$ Oe of $\text{PdBi}_{2-x}\text{Pb}_x$ with $x=0-0.35$ from 2K to 7K.

Similar consistent results were obtained through magnetic susceptibility measurements as shown in Fig. 3(b). The magnetization was measured under an applied magnetic field of 2 Oe on randomly oriented small crystals with typical mass ~ 20 mg packed in the gelatin capsules. All of the samples with doping level $0 < x < 0.35$ exhibit substantial diamagnetic shifts at the lowest temperature. The shielding fractions $4\pi\chi$ are close to or exceed 1 without the demagnetization factor correction, which implies the bulk superconducting nature of these samples. Consistent with the resistivity data, the superconducting transition temperature systematically moves downward with doping from 5.2K for $x=0$ to 2K for $x=0.40$.

To confirm the effective hole doping by Pb-substitution, Hall effect measurements have been carried out to evaluate the charge carrier concentration for the parent compound PdBi_2 and a representative Pb-doped $\text{PdBi}_{1.8}\text{Pb}_{0.2}$ sample (Fig. 4). The raw Hall resistivity ρ_H are linear with the field, with negative slopes for both samples. To further eliminate the effect of possible misalignment of Hall electrodes, the Hall coefficient R_H was taken as $R_H = [R_H(5T) + R_H(-5T)]/2$ at each temperature. The inset of Fig. 4 shows the Hall coefficient of PdBi_2 from 6K to 300K. The Hall coefficient is negative over the whole temperature range and only weakly depends on temperature, suggesting that the electron-type charge carriers dominate the charge transport. The value of Hall coefficient changes by $< 30\%$ from 2K to 300K, implying relatively minor multi-band effects, and therefore it is reasonable to evaluate the carrier concentration using the Hall coefficient R_H .

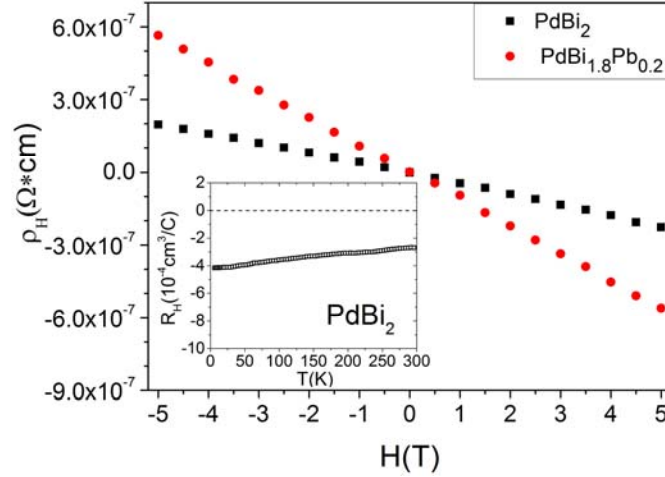


Fig.4 Hall resistivity of $\beta\text{-PdBi}_2$ and $\text{PdBi}_{1.8}\text{Pb}_{0.2}$ under magnetic field at 10K; the inset shows the Hall coefficient R_H of $\beta\text{-PdBi}_2$ from 6K to 300K.

The Hall resistivity of the parent compound and Pb-doped sample under different magnetic fields at 10K are shown in Fig. 4, where one can see that the contribution from magneto-resistance is rather small. The Hall coefficients R_H , determined by the slopes of the curves, are $R_H = -4.24 \times 10^{-4} \text{cm}^3/\text{C}$ and $R_H = -1.12 \times 10^{-3} \text{cm}^3/\text{C}$ for PdBi_2 and $\text{PdBi}_{1.8}\text{Pb}_{0.2}$, respectively. The negative Hall coefficient of the Pb-doped sample indicates that the charge carriers are still dominated by electrons. By simply using the single band expression $n = \frac{1}{R_H q}$, we can calculate electron concentrations: $n = 1.47 \times 10^{22} \text{cm}^{-3}$ for PdBi_2 and $n = 5.56 \times 10^{21} \text{cm}^{-3}$ for $\text{PdBi}_{1.8}\text{Pb}_{0.2}$. The substantial decrease of electron concentration suggests the effective hole-doping in the PdBi_2 system through Pb-substitution at the Bi site. This effective hole-doping might shift the Fermi level, resulting in a lower electronic density of states (DOS). Therefore, the lower DOS might contribute to the decrease of the T_c if a rigid band model is adopted.

Since the hole doping by Pb substitution caused the decrease of the T_c , we also attempted to carry out the Na-intercalation, which would introduce electrons into the system. Several trials with nominal Na-concentration ranging from $x=0.1$ to $x=0.4$ on Na_xPdBi_2 have been tested. X-ray powder diffraction analysis on the resulting bulk materials reveals that some small impurities (less than 10% total) of NaBi and Pd exist in the sample besides the formation of the β -tetragonal phase. We were able to isolate smaller pure crystals from the bulk samples and carried out detailed chemical analyses and physical measurements. The isolated crystals are homogeneous from WDS analysis and have all of the three elements present. However, the actual Na content is much lower than the nominal composition. Taking the nominal $x=0.1$ as an example, the actual composition we found from the chemical analysis was Na:Pd:Bi = 0.044(3):1:2.000(5). The highest Na doping level is $\sim 0.057(2)$ determined from the chemical analysis, indicating the relatively low limit of Na intercalation into this compound compared with the Pb-doping. The Na-doped crystals were moderately sensitive to air/moisture as they slowly decayed when kept outside of the glove box for one day. This also implies the successful Na-intercalation into the system. The superconducting T_c , on the other hand, is

rapidly suppressed at such a low Na-doping level, changing from 5.4K in PdBi_2 down to 4.1K in the $\text{Na}_{0.044}\text{PdBi}_2$, and further down to 3.9K in $\text{Na}_{0.057}\text{PdBi}_2$, as shown in the inset of Fig. 5(a). However, this is in great conflict with theoretical expectation,¹³ which suggests such electron-like doping should shift the Fermi level toward the DOS peak, increasing the DOS at the Fermi level and thus the T_c .

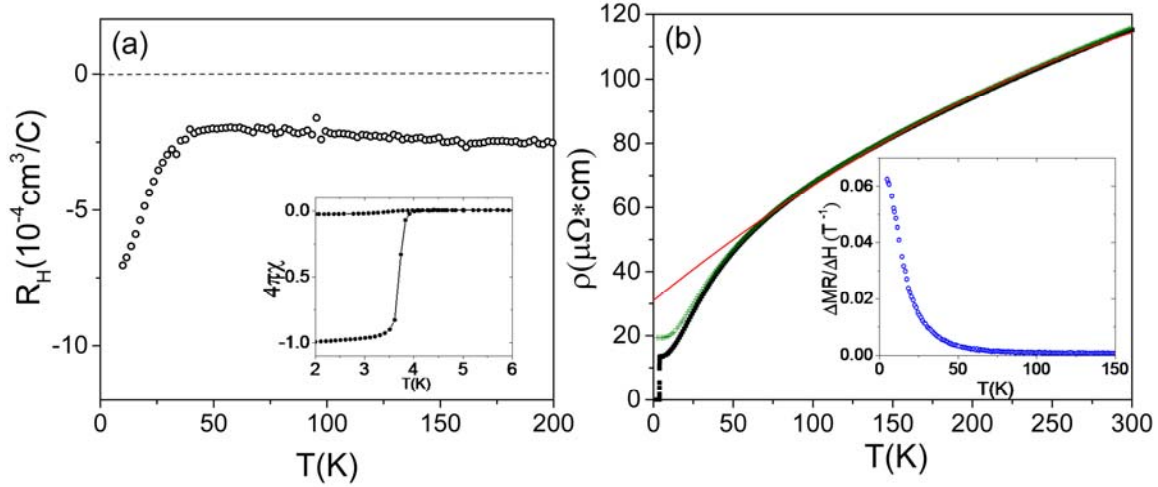


Fig.5 (a) The Hall coefficient R_H of $\text{Na}_{0.057}\text{PdBi}_2$ from 5K to 300K; the inset shows the magnetic susceptibility of $\text{Na}_{0.057}\text{PdBi}_2$. (b) Magnetoresistivity of $\text{Na}_{0.057}\text{PdBi}_2$ from 2K to 300K (solid black squares: zero field; green crosses: 7 T); The solid red line is only a guide for the eyes. The inset is the ratio of magnetoresistance ($\Delta\text{MR}=[\rho(7\text{T})-\rho(0\text{T})]/\rho(0\text{T})$) divided by the magnetic field.

To verify whether the DOS does increase through Na-intercalation, the Hall measurement was carried out on the $\text{Na}_{0.057}\text{PdBi}_2$ sample to probe the change of charge carrier concentration. Similar to that of PdBi_2 , the Hall coefficient R_H above 50K is T-insensitive for the Na-intercalated sample, as shown in Fig. 5(a). Therefore, the electron concentrations for PdBi_2 and $\text{Na}_{0.057}\text{PdBi}_2$ are calculated based on the R_H at 50 K as $1.58 \times 10^{22} \text{ cm}^{-3}$ and $3.09 \times 10^{22} \text{ cm}^{-3}$, respectively. There is apparently a significant increase of the carrier concentration, which is also in line with the decrease of the room-temperature resistivity observed in Fig. 5(b). The deduced $d\rho/dT$ at 300 K decreases from $0.37 \mu\Omega \cdot \text{cm}/\text{K}$ for PdBi_2 to $0.20 \mu\Omega \cdot \text{cm}/\text{K}$ for $\text{Na}_{0.057}\text{PdBi}_2$. The Na-intercalation, therefore, does introduce electrons and enhance the DOS as expected. The suppression of T_c has to be attributed to other mechanisms.

It is well known that both the competing excitations and the impurity scattering (especially pair-broken scattering) may suppress superconductivity. To explore the issue, both the magnetoresistance and the R_H are investigated (Fig. 5). The Hall coefficient R_H is enhanced almost by a factor of three with cooling below 50 K (Fig. 5a). As demonstrated previously (Fig. 4 inset), the multiband effect has trivial interferences on the R_H for the undoped PbBi_2 . The unexpected enhancement of the R_H in the Na-intercalated sample can hardly be attributed to the multiband effect, but is more likely caused by certain spin-related scattering/excitation. For example, Han *et al.* have

observed that the R_H of SrFeAsF significantly increased with cooling below 150-160 K with the spin-density-wave (SDW) transition around 173 K¹⁶. Such an interpretation seems to be supported by both the resistivity and the magnetoresistivity (Fig. 5(b)) data. However, It should be noted that these are rather general characteristics of all spin ordering/excitations. For instance, anomalous Hall effect and colossal magnetoresistance are observed in the manganites such as $La_{1-x}Ca_xMnO_3$ ^{17,18}. To explore the situation in $Na_{0.057}PdBi_2$, the $R(T)$ above 70 K is fitted as the quadratic function of T (the solid red line in Fig. 5(b)), where the R -drop below 50 K is evident. The $R(T)$ under magnetic field of 7 T, in particular, is much higher than that under 0 T (Fig. 5(b), inset) with the deduced $\frac{\partial \ln R}{\partial H} \approx 0.05/T$ at 10 K. The enhanced hump feature, the large magnetoresistance, and the increased amplitude of Hall coefficient below 50K suggest a Fermi surface reconstruction and excitation/ordering in the spin section around 50K induced by Na doping. Thus the suppressed superconductivity in Na-intercalated $PdBi_2$ could be attributed to the competing spin excitation associated with the Fermi surface reconstruction, although the exact nature of this spin excitations needs further investigation.

Based on the above data, we were able to construct the phase diagram of T_c as a function of doping level (both hole and electron doping) as shown in Fig. 6. At the right side of the phase diagram (hole doping), the T_c decreases continuously with the Pb-doping. The suppression of T_c can be understood as the decrease of DOS at the Fermi level caused by hole doping. At the left side of the figure, we demonstrate that the T_c is also quickly suppressed by a small amount of the Na-interclation. The cause of this T_c suppression could be attributed to the emergence of possible spin excitation, which may compete for the ground state and be counterproductive in stabilizing the superconducting state.

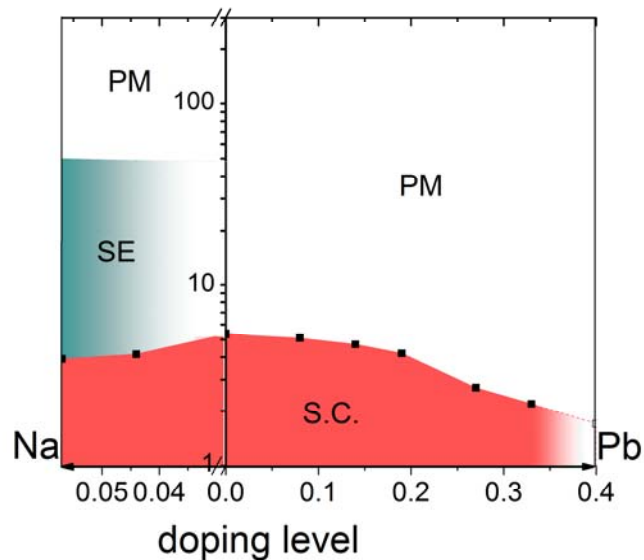


Fig.6 The phase diagram for both hole- and electron-doped $PdBi_2$. SC: superconducting transition temperature determined resistively; PM: paramagnetic state; “SE” possible spin excitation induced by Na-intercalation.

To further examine the above conjectures based on doping, we investigated the pressure effect on the undoped PbBi_2 with the highest T_c of this series by measuring temperature dependence of resistivity under pressures up to 16.63 kbar, as shown in Fig. 7. As the applied pressure increases, the normal state resistivity considerably decreases. A closer look at the low temperature part, as shown in Fig. 7(b), reveals that the superconducting transition becomes slightly sharper, and is gradually suppressed, upon the applied pressure at a linear suppression rate of $dT_c/dP = -0.28\text{K/GPa}$. At 16.63 kbar, the T_c is reduced to 4.9K. To verify the stability of the sample, the pressure cell was unloaded to lower pressure and ambient. The corresponding data are denoted as (u) in Fig. 7(b). We observed that superconducting transition T_c values measured upon loading and unloading the pressure cell fell along the same line, proving the stability of the sample in the pressure cycle. The corresponding phase diagram of T_c versus pressure is shown in the inset of Fig. 7(b). The suppression of T_c by pressures appears to be consistent with the doping experiment.

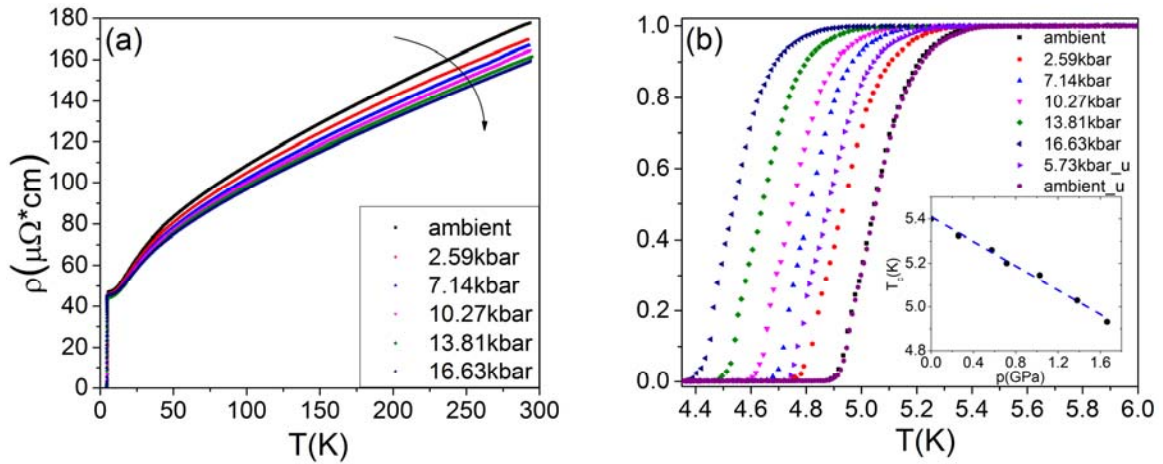


Fig.7 (a) The resistivity of $\beta\text{-PdBi}_2$ from 1.2K to 300K under high pressure. (b) The normalized resistivity under different pressures, where u denotes the unloaded pressure run. The inset shows the shift of T_c with pressure for $\beta\text{-PdBi}_2$.

Conclusions:

In summary, we have systematically grown large single crystals of layered compound $\beta\text{-PdBi}_2$, the hole-doped $\text{PdBi}_{2-x}\text{Pb}_x$ and the electron-doped Na_xPdBi_2 , and studied their magnetic and transport properties. Hall measurements on PdBi_2 , $\text{PdBi}_{1.8}\text{Pb}_{0.2}$, and $\text{Na}_{0.057}\text{PdBi}_2$ show that the charge transport is dominated by electrons in all of the samples. The electron concentration is substantially reduced upon Pb-doping in $\text{PdBi}_{2-x}\text{Pb}_x$ and increased upon Na-intercalation in Na_xPdBi_2 , indicating the effective hole-doping by Pb and electron-doping by Na. In Pb-doped PdBi_2 , we observed a monotonic decrease of T_c from 5.4K in undoped PdBi_2 to less than 2K for $x > 0.35$. The monotonic decrease of the T_c upon doping can be explained by the reduced DOS at the Fermi level.

In Na-intercalated samples, a rapid decrease of T_c with a slight Na-intercalation level is also observed, which is in contradiction with the theoretical expectation. Both the magnetoresistance and Hall measurements further reveal evidence for a possible competing spin excitation $\sim 50\text{K}$, which could contribute to the suppression of the T_c in Na-intercalated samples. Meanwhile, application of external pressure up to 16.63 kbar on the undoped PdBi_2 also suppresses the superconducting transition linearly with a dT_c/dP coefficient of -0.28K/GPa , consistent with the doping experiments.

References:

- [1] J. A. Wilson, F. J. Di Salvo, and S. Mahajan, *Adv. Phys.* **24**, 117 (1975).
- [2] G. Grüner, *Rev. Mod. Phys.* **60**, 1129 (1988).
- [3] C. dela Cruz, Q. Huang, J. W. Lynn, J. Li, W. Ratcliff, J. L. Zarestky, H. A. Mook, G. F. Chen, J. L. Luo, N. L. Wang, and P. C. Dai, *Nature* **453**, 899 (2008).
- [4] X. F. Wang, T. Wu, G. Wu, H. Chen, Y. L. Xie, J. J. Ying, Y. J. Yan, R. H. Liu, and X. H. Chen, *Phys. Rev. Lett.* **102**, 117005 (2009).
- [5] H. Zhang, C. X. Liu, X. L. Qi, X. Dai, Z. Fang, and S. C. Zhang, *Nat. Phys.* **5**, 438 (2009).
- [6] Y. Zhang, K. He, C. Z. Chang, C. L. Song, L. L. Wang, X. Chen, J. F. Jia, Z. Fang, X. Dai, W. Y. Shan, S. Q. Shen, Q. Niu, X. L. Qi, S. C. Zhang, X. C. Ma, and Q. K. Xue, *Nat. Phys.* **6**, 584 (2010).
- [7] J. Nagamatsu, N. Nakagawa, T. Muranaka, Y. Zenitani, and J. Akimitsu, *Nature (London)* **410**, 63 (2001).
- [8] S. Yamanaka, H. Kawaji, K. Hotehama, and M. Ohashi, *Adv. Mater.* **8**, 771 (1996).
- [9] N. N. Zhuravlev, *Zh. Eksp. Teor. Fiz.* **32**, 1305 (1957).
- [10] H. Okamoto, *J. Phase Equilib.* **15**, 191 (1994).
- [11] B. T. Matthias, T. H. Geballe, and V. B. Compton, *Rev. Mod. Phys.* **35**, 1 (1963).
- [12] Y. Imai, F. Nabeshima, T. Yoshinaka, K. Miyatani, R. Kondo, S. Komiya, I. Tsukada, and A. Maeda, *J. Phys. Soc. Jpn.* **81**, 113708 (2012).
- [13] E. Herrera, I. Guillamon, J.A. Galvis, A. Correa, A. Fente, R.F. Luccas, F.J. Mompean, M. Garcia-Hernandez, S. Vieira, J.P. Brison and H. Suderow, *Arxiv*: 1506.01411(2015).
- [14] I. R. Shein and A. L. Ivanovskii, *J. Supercond. Nov. Magn.* **26**, 1 (2013).

[15] C. W. Chu, *Phys. Rev. Lett.* **33**, 1283 (1974).

[16] F. Han, X. Zhu, G. Mu, P. Cheng, and H. H. Wen, *Phys. Rev. B* **78**, 180503 (2008).

[17] P. Schiffer, A. P. Ramirez, W. Bao and S-W. Cheong, *Phys. Rev. Lett.* **75**, 3336 (1995).

[18] P. Matl, N. P. Ong, Y. F. Yan, Y. Q. Li, D. Studebaker, T. Baum, and G. Doubinina, *Phys. Rev. B* **57**, 10248 (1998).